PURPOSE-LED
PUBLISHING™

PAPER • OPEN ACCESS

The impacts of three PBL schemes on the simulation of boundary layer meteorological factors and air pollutants in Northern China

View the article online for updates and enhancements.

The impacts of three PBL schemes on the simulation of boundary layer meteorological factors and air pollutants in Northern China

Jikang Wang[1], Bihui Zhang, Hengde Zhang and Mengyao Lv

National Meteorological Center of CMA, China Meteorological Administration, Beijing, China.

[1] Email:wjk_1990@16.com

Abstract. Three planetary boundary layer (PBL) schemes (YSU, MYJ, ACM2) were applied in the WRF-CAMx model to simulate the meteorology variables and air pollutants over Beijing-Tianjin-Hebei region in Northern China in November 2015. The simulated meteorological factors near the surface , and air pollutants were evaluated by observations. All the three PBL schemes overestimated the wind speed in the lower atmosphere and underestimated the 2-m temperature and humidity. The MYJ scheme produced the largest biases on the 10-m wind speed (+1.2 m/s), and the YSU and ACM2 schemes produced similar results. The critical Kv method, which based on the vertical diffusivities, was used to recalculate the model PBL heights. The MYJ scheme gave the lowest PBL heights among the three schemes using the critical Kv method, and then it produced the highest air pollutants concentrations. The YSU and ACM2 schemes produced similar air pollutant concentrations, and the mean concentrations were about 6~10% less than the MYJ simulations. The stronger surface wind produced by the MYJ scheme decreased the air pollutant concentrations (about 2%).

1. Introduction

Due to the industrialization and urbanization in the past few decades, the Beijing-Tianjin-Hebei (BTH) region has been regarded as one of the most severe haze region in China[1,2]. The heavy pollution is correlated with the high anthropogenic emissions in the BTH region [3,4]. In addition to high emission, synoptic patterns and meteorological factors also play an important role in the formation of the frequent haze pollution in this region[5,6,7] .

The atmospheric boundary layer structure and surface meteorological elements are important meteorological factors that affect the formation and dissipation of air pollutants[8,9]. Accurate simulation of the meteorological factors within planetary boundary layer is critical for correctly simulating air quality [10]. PBL schemes are provided to parameterize the boundary layer structure in mesoscale meteorological models. The PBL schemes adopt diverse assumptions regarding the turbulence, which lead to different characters in the boundary layer. Several PBL schemes have been assessed in the weather research forecasting model (WRF)[11,12]. Hu (2010) found that difference in performances of various schemes were dominantly due to variation in vertical mixing strength and entrainment of the air form above the PBL[11].

Several studies have examined the impact of PBL schemes on simulating air quality [12,13]. Li et al. (2016) simulated the severe haze in China using the WRF-Chem model and compared the influence

of three PBL schemes (YSU, MYJ, Boulac) in the surface $PM_{2.5}$ concentration. All three schemes performed better in simulating the daily average variation trends than diurnal variations of surface $PM_{2.5}$ and little difference was found in simulation with three schemes[12]. Therefore, more studies need to be conducted on the PBL parameterizations in haze days to get a better haze forecasting.

Three PBL schemes (YSU, MYJ, ACM2) in the WRF model were selected to simulate the meteorological factors in our study. The Comprehensive Air Quality Model with Extensions (CAMx) was used to simulate the $PM_{2.5}$ with respect to each meteorological set. We focused on the difference between the haze days and clean days in Beijing-Tianjin-Hebei region in November 2015. The surface meteorological factors were used to evaluate the performances in the meteorological fields of the three schemes. The vertical diffusivity was analyzed to get more details about how the three PBL schemes influence the dispersion process in the air quality model.

2. Data and methodology

2.1. Model configuration
In this study we used the WRF model version 3.5.1 to develop meteorological fields. Initial and lateral boundary conditions were determined using the National Centers for Environmental Prediction (NCEP) final (FNL) operational global analyses. The physical parameterization options included Dudhia shortwave radiation[14], RRTM longwave scheme[15],and the Unified Noah land-surface scheme [16].

The CAMx model verison 6.2 was used to simulate air pollutants with SAPRC99 gas phase chemistry [17]. The aerosol chemistry was described using a coarse-fine (CF) scheme. The anthropogenic emissions data for gaseous and particulate pollutants were derived from the Multiresolution Emission Inventory of China (MEIC, http://www.meicmodel.org). The latest available emission data in MEIC with real statistics was for 2012. In our study, the emission data of 2015 was extrapolated from the MIEC emission data of 2012 according to the brief statistics. The biogenic emissions are computed from the Biogenic Emissions Inventory System version 3 (*BEIS3*) within the Sparse Matrix Operator Kernel Emissions (*SMOKE*) modelling system (SMOKE) model.

Two-way nesting domains were configured in the WRF model with grid spacing of 24 km and 8 km, respectively. The outer domain covers the mainland of China, and the inner domain contains the BTH region and its surrounding region, as shown in Figure 1. All the WRF model domains have 35 vertical layers and the top is set at 50 hPa. The lowest model sigma levels at 1.0, 0.9975, 0.995, 0.99, 0.98, 0.97, 0.96, 0.94, 0.92, 0.90, 0.875, and 0.85. The CAMx model domains share the same grid spacing as the WRF model and the scales are less than the WRF model by 5 grid cells at each side. The CAMx model has 22 vertical layers and the lowest 12 layers are the same as the WRF model.
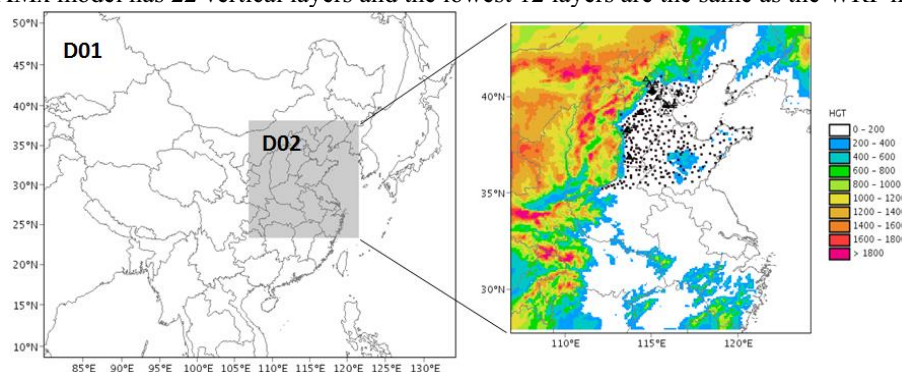
Figure 1. I The model domain and the location of the weather stations (the black dot) and the air quality monitoring stations (the triangle), the color shaped is the altitude above sea surface.

2.2. Three PBL schemes

PBL schemes are used to characterize the boundary layer structure and to describe the vertical fluxes of heat, momentum, moisture within PBL and throughout the atmosphere in the turbulent processes. The PBL schemes can be classified into two types, the local closure scheme and the non-local scheme. The local closure scheme calculates the turbulent fluxes using the mean variables and their gradients at each model grid. The non-local closure scheme also considered the fluxes generated from large eddy under convective conditions. In our study, three PBL schemes were selected to simulate the meteorological fields.

The Yonsei University (YSU) PBL scheme is a first order non-local scheme. It is based on the theory of molecular diffusion (K-theory). The PBL height is diagnosed using a critical bulk Richardson.. In the YSU scheme, vertical diffusivity (K) within the PBL is calculated by using the PBL height and the relationship of the Prandtl number (Pr)[18] .

The MYJ PBL scheme is a 2.5 order turbulence local closure scheme. It determines eddy diffusion coefficients by calculating turbulent kinetic energy (TKE). The PBL height is defined as the height of the lowest model level at which the TKE is unable to balance the dissipation[19]. The vertical diffusivity (K) is defined by the turbulence kinetic energy and the stability corrected variable.

The Asymmetrical Convective Model version 2 (ACM2) PBL scheme is a first-order closure scheme. The scheme diagnoses the PBL height by using a critical bulk Richarson (0.25) as the YSU scheme. It features non-local upward mixing and local downward mixing. The scheme shuts off nonlocal transport for stable or neutral flow [20].

The vertical diffusivity in the air quality model (CAMx) used to mix air pollutants is taken to be the diffusivity of heat in the WRF model. Then CAMx can calculate the vertical diffusivity from the output of the WRF model. The ACM2 parameterization has been implemented in CAMx as an alternative to the K-theory approach. CAMx uses the standard K-theory to describe the vertical diffusion process when the ACM2 option is set off [17]. In our study, the K-theory was used by YSU and MYJ scheme and the ACM2 parameterization was used for ACM2 scheme. The K-theory diffusion is defined as following.

$$\frac{\partial c}{\partial t} = \frac{\partial}{\partial z}\left[\rho K \frac{\partial (c/\rho)}{\partial z}\right] \tag{1}$$

Where c is the air pollutants concentration, t is the time, z is the height of each layer, ρ is the atmospheric density, K is the vertical diffusion.

2.3. Evaluation data

The meteorological observations were from the China Metrological Administration. 106 surface weather stations in BTH were used to evaluate the simulated 10m wind, humidity and temperature at 2m from the mode (locations depicted in Figure 1). The air quality data for November 2015, including the hourly $PM_{2.5}$ are from the China National Environmental Monitoring Center. We selected 65 monitoring stations in the BTH region to evaluate the air quality model.

When the daily averaged $PM_{2.5}$ concentrations were above $75\mu g/m^3$ in most cities (especially in Beijing, Tianjin, Shijiazhuang) of the BTH region, we considered that an air pollution event occurred. There were 3 pollution processes hitting the BTH region in November 2015. The first episode was from November 2nd to 5th. The second episode lasted from November 10th to 15th. The third episode was from November 27th to 30th.

Table 1. Definition of statistics metrics.

Metrics	Definition
MB (Mean Bias)	$MB = \frac{1}{n}\sum_{1}^{n}(C_m - C_o)$
RMSE (Root mean square error)	$RMSE = \sqrt{\frac{1}{n}\sum_{1}^{n}(C_m - C_o)^2}$
IOA (Index of agreement)	$IOA = 1 - \frac{\sum_{1}^{n}(C_m - C_o)^2}{\sum_{1}^{n}(|C_m - \overline{C_o}| + |C_o - \overline{C_o}|)^2}$

Note: C_m is the model simulated value, C_o is the observed value, and n is the number of prediction–observation pairs drawn from all monitoring stations. $\overline{C_o}$ is the average observed value.

3. Evaluation of WRF meteorology

Meteorology variables were evaluated by means of mean bias (MB), root of mean square error (RMSE), and index of agreement (IOA) (Table 1). The IOA varies between 0 and 1. A value of 1 indicates a perfect match, and 0 indicates no agreement [21]. Wind direction was evaluated by the angle between the predicted direction and the observed direction rather than the mean bias.

3.1. Surface meteorology variables

The 2-m air temperature (T2), 10-m wind speed and direction and humidity are critical variables to simulate air pollutants in air quality model. In this study, these surface meteorological variables are used to compare the WRF model-simulated results from 106 weather observations. Table 2 shows the MB, RMSE and IOA between WRF simulated meteorological factors and the observations.

All the three PBL schemes overestimated the 10 m-wind speed. The ACM2 and the YSU performed better than the MYJ at 10m-wind speed with the less MB (0.71, 0.51 and 1.22 m/s for the ACM2, the YSU and the MYJ). The angles between the predicted and the observed 10m-wind direction were 37.49, 37.91 and 36.70°for the ACM2, the YSU and the MYJ, respectively. All the three PBL schemes underestimated the 2m-temperature and the 2m-humidity. The MBs of the MYJ scheme on T2 and humidity is -0.32 K and -0.28 g/kg respectively, which were the least underestimations among the three PBL schemes.

Generally, the ACM2 and the YSU had the similar performance on the surface meteorological variables. Compared to the ACM2 and the YSU, MYJ had smaller under-prediction on T2 and humidity and bigger overestimation on 10-m wind speed. Hu et al. evaluated the three PBL schemes using the surface observation in Texas, and found the three PBL schemes underpredicted the T2 with -1.25 to -0.63 K [11]. The underestimation of T2 in our study was better than the results in Hu et al (2010). However, their results indicated the MYJ scheme produced the coldest biases, which is different from ours. The 10-m wind was overestimated by the WRF model, which was consistent with previous studies [22,23].

Table 2. Statistical metrics of simulated and observed surface meteorological variables

|	MB			RMSE			IOA		
	ACM2	YSU	MYJ	ACM2	YSU	MYJ	ACM2	YSU	MYJ
10-m Wind Speed(m/s)	0.71	0.51	1.22	1.5	1.41	1.79	0.65	0.65	0.63
10-m Wind Direction (°)	37.49	37.91	36.7						
2-m Temperature(K)	-0.62	-0.68	-0.32	2.46	2.52	2.51	0.89	0.89	0.88
2-m Humidity (g/kg)	-0.39	-0.36	-0.28	0.68	0.67	0.64	0.82	0.82	0.83

The MB for wind direction was the angle between the predicted and the observed wind direction. Humidity was given as water vapor mixing ratio.

We defined the weather conditions with low visibility (less than 5 km) and low relative humidity (less than 90%) as haze conditions and those with high visibility (more than 10 km) weather conditions as clean conditions[24] . The three PBL scheme performances in clean and haze conditions are showed in table 3. The three schemes did not perform as well in haze conditions as in clean conditions on the 10-m wind. The model undervalued the water vapour during the haze days more than the clean days. The underestimation of the model simulated 2-m temperature under haze conditions were less than in the clean conditions. Compared to the MBs of T2 in table 1, the MYJ performance changed a lot. The MYJ hold the coldest biases during the clean conditions which was consistent with other studies [11,25]. The overestimation of MYJ on the temperature during the haze

conditions led to the good performance on the average of MB in table 1. Figure 2 shows the diurnal variations of the MB of 2m-Temperature and 2m-Humidity. In the daytime, all the three PBL schemes overpredicted the T2 on haze days. An explanation for this finding is that reduced the incoming solar radiation via backscattering more than simulated on these days[26].

Table 3. The MB of the surface meteorological variables in haze days and clean days

	CLEAN			HAZE		
	YSU	MYJ	ACM2	YSU	MYJ	ACM2
10-m wind speed	0.08	1.09	0.39	0.61	1.17	0.75
10-m wind direction	30.76	28.72	29.51	40.91	40.42	40.85
2-m temperature	-1.43	-1.45	-1.37	-0.22	0.25	-0.21
2-m humidity	-0.09	-0.02	-0.13	-0.44	-0.36	-0.47
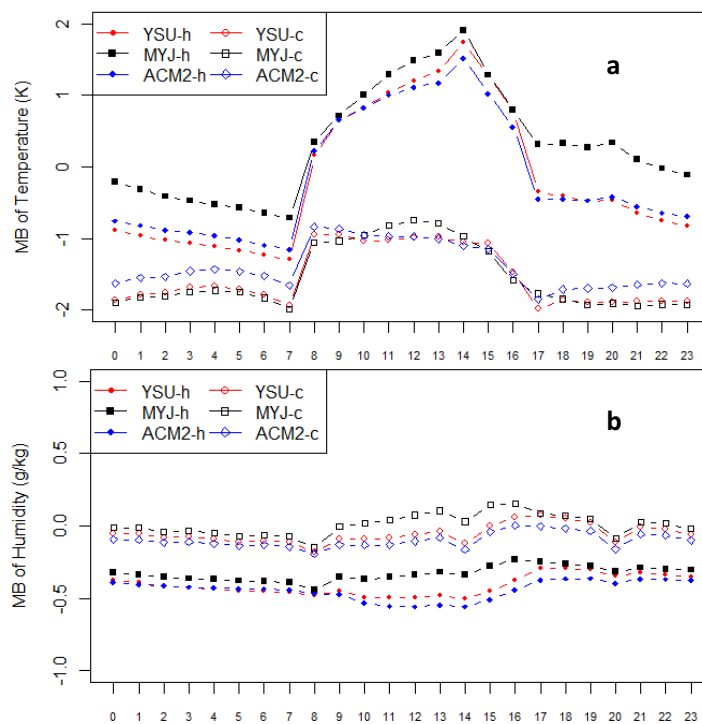
Figure 2. Mean diurnal variations of the MB of 2m-temperature (a) and 2m-humidity (b), filled dots (YSU-h, MYJ-h, ACM2-h) indicate results for haze days and open dots (YSU-c, MYJ-c, ACM2-c) for clean days.

3.2. PBL height

Different methods were used to determine the PBL height in different PBL schemes, which may cause variation in PBL heights even if the simulations were accurate. The PBL height influences the vertical distribution of air pollutants through influencing the vertical diffusivity as described in section 2.2. The CAMx model provides another method (the critical Kv method) to redefine the PBL height based on the vertical diffusivity. They define the top of the PBL as the height where the vertical diffusivity (Kv) decreases to a critical value. The critical value is the minimum Kv needed for a well-mixed model layer with arbitrary layer depths. Starting with an initial un-mixed mixing ratio distribution (1

and 0 units, respectively) among two adjacent layers of different and arbitrary thickness, the critical Kv results in a final mixing ratio distribution of 2/3 and 1/3 units in 2/3 of an hour. Therefore, the PBL height determined by the critical Kv characterizes the vertical diffusion of air quality in the PBL directly. The critical Kv is defined as follows:

$$Kv = 0.03dz1\,(dz1 + dz2)/200 \qquad (2)$$

where dz1 and dz2 are the depths of arbitrary two adjacent layers

Figure 3 shows the monthly average of PBL heights over northern china derived from WRF model and the critical Kv method. According to results of the WRF model, the PBL height diagnosed by the MYJ was above 400 m over BTH region and it was higher than the PBLH produced by the ACM2 and YSU. The PBL heights determined by the critical Kv method were lower than the PBL heights from the WRF model. The PBL heights decreased about 50~100m, 50~100m and 200 ~250m for the YSU, ACM2 and MYJ respectively. Then the MYJ gave the lowest PBL heights using the critical Kv method among the three schemes. Therefore, the difference in diagnosed PBL heights of the different PBL schemes may not reflect their differences in the vertical diffusion of air pollutants.

The diurnal variables of the PBL heights derived from the model were compared with the PBL hights determined by the Nozaki method (Figure 4). The Nozaki method is based on surface meteorological observations of temperature, dew point, wind speed and the Pasquill stability classification[27]. For the YSU and ACM2 scheme, the PBL heights using the critical Kv method were lower than the original in the afternoon and the night time. For the MYJ scheme, the PBL heights were lower during all the day. The max height produced by the YSU and ACM2 was similar to that by the Nozaki method. The max height produced by MYJ was much lower from the critical Kv method. The max heights given by the YSU and ACM2 were consistent with the observed values reported by other studies [5, 8]. At the 17:00 and 20:00 Beijing time, the PBL heights given by the model were much lower than the Nozaki method. Compared with the daily minimum PBL height (238±202m) reported by Tang et al. (2016)[8], the model gave much lower heights (160 m from the WRF model and 86 m from the critical Kv method) in the nighttime.
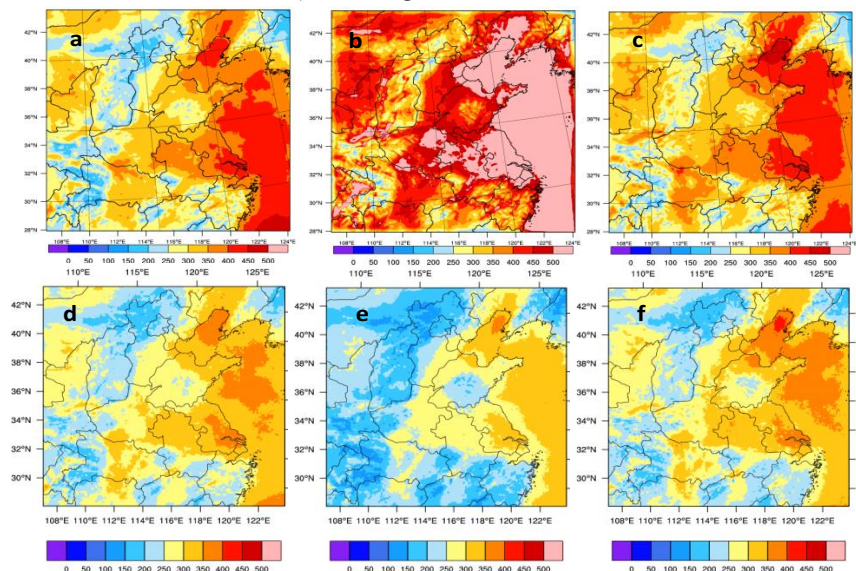
Figure 3. The monthly average of PBL height derived from the YSU(a), the MYJ(b), the ACM2(c) scheme and the redefined PBL height using Kv derived from the YSU(d), thr MYJ(e), the ACM2(f).
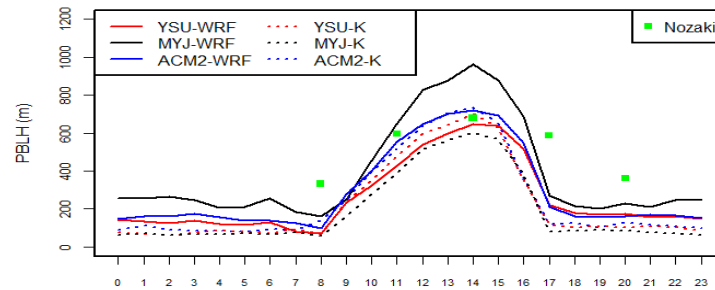
Figure 4. The PBL heights at Beijing derived from the WRF model out (YSU-WRF, MYJ-WRF, ACM2-WRF), the the critical Kv (YSU-K, MYJ-K, ACM2-K) and Nozaki method.

4. Impact of PBL modelling on the results of air quality model

4.1. The impact on the vertical diffusion

The PBL heights affected the diffusion of air pollutants, by influencing the distribution of vertical diffusivities. We analyzed the difference of vertical diffusivities among the three PBL schemes (Figure 5). The vertical diffusivities derived from the three PBL schemes within the PBL were much bigger than above the PBL. The max vertical diffusivities occurred at level 5 at noon. The ACM2 hold larger vertical diffusivities than other two schemes near the top of PBL, because the ACM2 determined the vertical diffusivities using the local scheme near the top of the PBL [20]. At the top of the PBL, the local scheme produced a bigger vertical diffusivity than the non-local scheme. The vertical diffusivity determined by YSU during the daytime were larger than other two schemes at the low level (level 0-4) layers and above level 10, but were less from the level 4 to level 8.
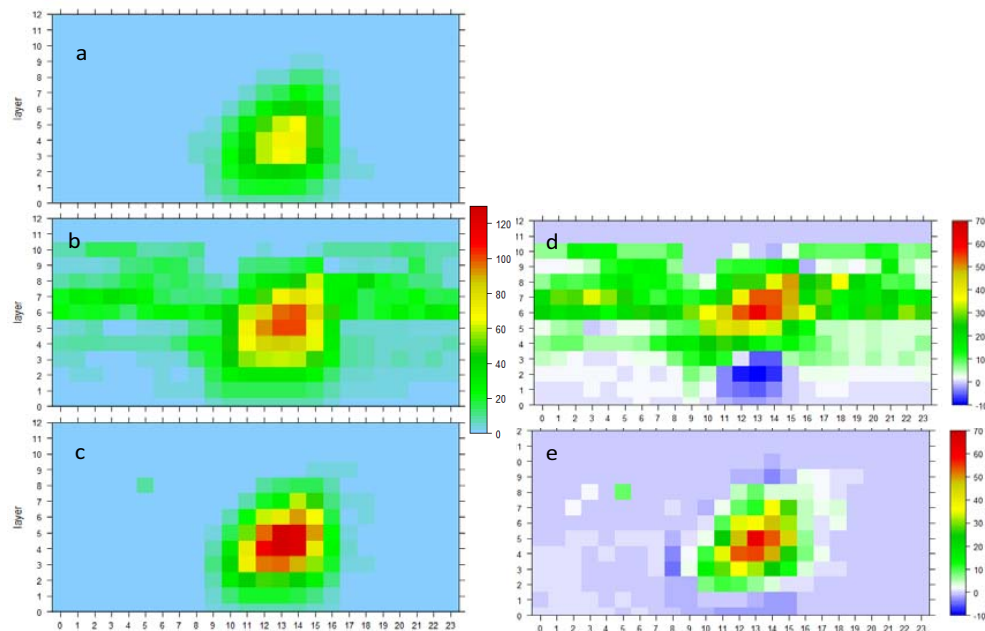
Figure 5. The monthly average of the diurnal cycle of vertical diffusivities for the YSU (a), the ACM2 (b), and the MYJ (c), and the difference among the three schemes (d: ACM2-YSU, e: MYJ-YSU). The sigma levels of the layers were at 1.0, 0.9975, 0.995, 0.99, 0.98, 0.97, 0.96, 0.94, 0.92, 0.90, 0.875, and 0.85.

4.2. The impact on the air pollutants simulation

The MYJ hold the highest concentration among the three PBL schemes for all four pollutants considered in this study as shown in Table 4. The model performed well on the mean concentrations of air pollutants except SO_2. The overestimation to SO_2 should be attributed to the uncertainties of emissions. In the section 3.2, the MYJ produced the lowest PBL height using the critical Kv method. Therefore, the low PBL height should be the main reason for the high air pollutants for the MYJ. The ACM2 and the YSU schemes had the similar results, because of the similar PBL heights. Although the ACM2 scheme had slightly lower PBL heights than the YSU scheme, the results of ACM2 was not consistent with the PBL heights, since the ACM2 scheme used the ACM2 parameterization to describe the vertical diffusion rather than the K-theory.

MYJ gave stronger wind on the surface (section 3.1). We used the meteorological fields from MYJ and the vertical diffusivities calculated using the YSU and the ACM2 method (section 2.2) to simulate the air pollutants (Table 4, MYJ-YSU and MYJ-ACM2). The mean concentrations from MYJ-YSU were only slightly lower (~2%) than the original YSU.

Table 4. The statistic metrics of the simulated and observed $PM_{2.5}$, SO_2, NO_2, CO at 65 stations in BTH region using different PBL schemes

	$PM_{2.5}$			SO_2			NO_2			CO		
Mean(obs)	93.14 μg/m³			35.22 μg/m³			55.87 μg/m³			1.88 mg/m³		
Metrics	SIM	RMSE	IOA	SIM	RMSE	IOA	SIM	RMSE	IOA	SIM	RMSE	IOA
YSU	85.79	50.92	0.57	74.03	55.59	0.39	55.87	27.93	0.54	1.52	1.44	0.44
ACM2	82.52	51.91	0.55	77.12	70.33	0.39	57.01	26.78	0.55	1.55	1.38	0.46
MYJ	90.54	52.75	0.55	79.31	71.482	0.38	60.31	27.74	0.54	1.71	1.44	0.44
MYJ-YSU	85.27	51.71	0.55	74.03	55.54	0.41	55.77	26.57	0.55	1.45	1.42	0.44
MYJ-ACM2	83.84	50.41	0.57	74.15	55.52	0.41	55.33	26.27	0.55	1.48	1.49	0.46

Note: the Mean (OBS) is the observed mean concentration at the stations. SIM is the mean concentration from the model using different PBL schemes. The MYJ-YSU and MYJ-ACM2 simulate the air pollutants using the meteorological fields from MYJ PBL scheme and the vertical diffusivities produced by the YSU and the ACM2 method.

Figure 6 shows the diurnal variations of observed and modelled $PM_{2.5}$ concentrations in the clean and haze days. The MYJ scheme produced highest concentrations of all the air pollutants among the three schemes, because MYJ gave the lowest PBL heights using the critical Kv method. The YSU scheme gave lower concentrations than the ACM2 schemes during the haze days, because the YSU produced higher PBL heights than the ACM2. The YSU gave slightly higher concentrations than the ACM2 during the clean days because the ACM2 scheme used the local closure way to calculate the vertical diffusivities in the neutral conditions. The local way calculated larger Kv than the no-local way when there were strong wind shears in the neutral conditions.
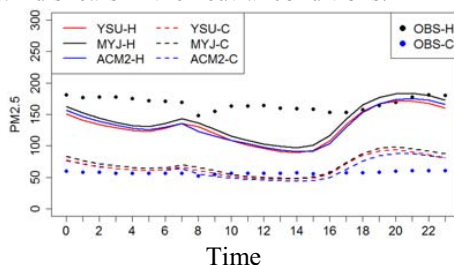
Figure 6. The diurnal variations of air pollutants in haze days and clean days (YUS-H, MYJ-H and ACM2-H are the simulated air pollutants using the YSU, the MYJ and the ACM2 schemes in haze days. YUS-C, MYJ-C and ACM2-C are in the clean days. OBS-H and OBS-C are the observed air pollutants in haze days and clean days.).

5. Conclusions

Three PBL schemes (the YSU, the MYJ, and the ACM2) were applied in the WRF-CAMx model to simulate the meteorology variables and air pollutants over Beijing-Tianjin-Hebei (BTH) region in November 2015. Weather stations observations data and air quality data were used to evaluate the model results. The differences among the model results of the three PBL schemes and the difference between haze days and clean days were analyzed in our study.

The WRF simulation indicated that all the three PBL schemes overestimated the 10-m wind speed (0.51~1.22m/s) and underestimated the 2-m temperature (-0.68 ~ -0.32) and humidity (-0.39 ~ -0.28). The MYJ scheme gave the largest biases on the 10-m wind speed and the least biases on the 2-m temperature and humidity. The YSU and ACM2 schemes produced similar results on the surface meteorology variables. All the three PBL schemes produced higher 2-m temperature and lower water mix ratio during haze conditions than during clean conditions.

The critical Kv method, which based on vertical diffusivities, was used to recalculate the PBL heights using the model results. The MYJ gave the lowest the PBL heights using the critical Kv method, while it gave the highest PBL heights using the original way. The model produced lower PBL heights during the nighttime than the observed results reported in other studies.

The MYJ scheme produced the highest air pollutants concentrations among the three PBL schemes, which were verified by that the MYJ produced the lowest PBL heights using the critical Kv method. The ACM2 and YSU scheme gave the similar simulated air pollutants, and the mean concentrations were about 6~10% less than the MYJ simulations. The PBL heights determined by the critical Kv method could reflect the vertical diffusion better than other methods. Overestimated surface winds produced by the MYJ scheme decreased the air pollutant concentrations (about 2%). The effects of systemically overestimated wind speed on air pollutants simulation in lower atmosphere need further studies.

References

[1]   Huang R J, Zhang Y, Bozzetti C, Ho K F, Cao J J, Han Y, Daellenbach K R, Slowik J G, Platt S M, Canonaco F, Zotter P, Wolf R, Pieber S M, Bruns E A,Crippa M, Ciarelli G, Piazzalunga A, Schwikowski M, Abbaszade G, Schnelle-Kreis J, Zimmermann R, An Z, Szidat S, Baltensperger U, El Haddad I, Prévôt A 2014 High secondary aerosol contribution to particulate pollution during haze events in china *Nature* **514(7521)** 218

[2]   Chai F, Gao J, Chen Z, Wang S, Zhang Y, Zhang J, Zhang H, Yun Y, Ren C 2014 Spatial and temporal variation of particulate matter and gaseous pollutants in 26 cities in china *J Environ Sci china* **26(1)** 75-82

[3]   Zhao B, Wang P, Ma J Z, Zhu S, Pozzer A, Li W 2012 A high-resolution emission inventory of primary pollutants for the Huabei region, China, *Atmos Chem Phys* **12(1)** 481–501

[4]   Lu Z, Streets D G, Zhang Q, Wang S, Carmichael G R, Cheng Y F, Wei C, Chin M, Diehl T, Tan Q 2010 Sulfur dioxide emissions in China and sulfur trends in East Asia since 2000, *Atmos Chem Phys* **10(13)** 6311–6331

[5]   Li M, Tang G Q, Huang J, Liu Z R, An J L, Wang Y S 2015 Characteristics of Winter Atmospheric Mixing Layer Height in Beijing-Tianjin-Hebei Region and Their Relationship with the Atmospheric Pollution *Environmental Sciences* **36(6)** 1935

[6]   Hu X, Ma Z, Lin W, Zhang H, Hu J, Wang Y, Xu X B, Fuentes J D, Xue M 2014 Impact of the Loess Plateau on the atmospheric boundary layer structure and air quality in the North China Plain: A case study *Sci Total Environ* **499** 228–237

[7]   Zhang Z, Zhang X, Gong D, Quan W, Zhao X, Ma Z, Kim S J 2015 Evolution of surface O3 and PM25 concentrations and their relationships with meteorological conditions over the last

decade in Beijing, *Atmos Environ* **108** 67–75

[8]   Tang G, Zhang J, Zhu X, Song T, Munkel C, Hu B, Schafer K, Liu Z X, Zhang J, Wang L, Xin J, Suppan P, Wang Y 2016 Mixing layer height and its implications for air pollution over Beijing, China *Atmos Chem Phys* **16(4)** 2459-2475

[9]   Aron R H 1983 Mixing height - an inconsistent indicator of potential air pollution concentrations *Atmos Environ* **17(11)** 2193-2197

[10] Zhang F, Bei N, Nielsengammon J W, Li G, Zhang R, Stuart A L, Aksoy A 2007 Impacts of meteorological uncertainties on ozone pollution predictability estimated through meteorological and photochemical ensemble forecasts *J Geophys Res* **112** D04304

[11] Hu X, Nielsengammon J W, Zhang F 2010 Evaluation of Three Planetary Boundary Layer Schemes in the WRF Model *Journal of Applied Meteorology and Climatology* **49(9)** 1831-1844

[12] Li T, Wang H, Zhao T, Xue M, Wang Y, Che H, Jiang C 2016 The Impacts of Different PBL Schemes on the Simulation of PM25 during Severe Haze Episodes in the Jing-Jin-Ji Region and Its Surroundings in China *Advances in Meteorology* 2016 1-15

[13] Banks R F, Baldasano J M 2016 Impact of WRF model PBL schemes on air quality simulations over Catalonia, Spain *Sci Total Environ* 98-113

[14] Dudhia J 1989 Numerical study of convection observed during the winter monsoon experiment using a mesoscale two dimensional model *J Atmos Sci* **46** 3077–3107

[15] Mlawer E J, Taubman S J, Brown P D, Iacono M J, Clough S A 1997 Radiative transfer for inhomogeneous atmospheres: RRTM, a validated correlated-k model for the longwave *J Geophys Res*, 102D **16** 663–16 682

[16] Tewari M, Chen F, Wang W, Dudhia J, Lemone M A, Mitchell K E, Michael E K, Gayno G, Wegiel J W, Guenca R 2004 Implementation and verification of the unified Noah land-surface model in the WRF model [presentation] 20th Conference on Weather Analysis and Forecasting/16th Conference on Numerical Weather Prediction, American Meteorological Society, Seattle, WA, US

[17] ENVIRON, 2015 User's guide to the Comprehensive Air Quality Model with Extensions (CAMx) Version 52 Available at: http://www.camx.com

[18] Hong S Y, Noh Y, Dudhia J 2006 A new vertical diffusion package with an explicit treatment of entrainment processes *Mon Weather Rev* **134 (9)** 2318–2341

[19] Mellor G L, Yamada T 1982 Development of a turbulence closure model for geophysical fluid problems *Rev Geophys* **20** 851–875

[20] Pleim JE 2007 A combined local and nonlocal closure model for the atmospheric boundary layer Part I: model description and testing *J Appl Meteorol Climatol* **46 (9)** 1383–1395

[21] Willmott C J 1981 On the validation of models *Physical Geography* **2** 184–194

[22] Shimada S, Ohsawa T, Chikaoka S, Kozai K 2011 Accuracy of the Wind Speed Profile in the Lower PBL as Simulated by the WRF Mode Sola 109-112

[23] Akylas E, Kotroni V, Lagouvardos K 2007 Sensitivity of high-resolution operational weather forecasts to the choice of the planetary boundary layer scheme *Atmospheric Research* **84(1)** 49-57

[24] Che H C, Zhang X, Wang Y, Zhang L, Shen X, Zhang Y, Ma Q L, Sun J Y, Zhang Y, Wang T 2016 Characterization and parameterization of aerosol cloud condensation nuclei activation under different pollution conditions *Sci Rep* **6(1)** 24497-24497

[25] Zhang Y, Gao Z, Li D, Li Y, Zhang N, Zhao X, Chen J 2014 On the computation of planetary boundary-layer height using the bulk Richardson number method *Geosci Model Dev* **7(6)** 2599-2611

[26] Jacobson MZ 1998 Studying the effects of aerosols on vertical photolysis rate coefficient and temperature profiles over an urban airshed *J Geophys Res* **103** 10593-10604

[27] Nozaki KY 1973 Mixing Depth Model Using Hourly Surface Observations, Report 7053, USAF Environmental Technical Applications Center